Int J Earth Sci (Geol Rundsch)
DOI 10.1007/s00531-010-0570-x

ORIGINAL PAPER

Magnetostratigraphy and paleomagnetism of early and middle Miocene synorogenic strata: basement partitioning and minor block rotation in Argentine broken foreland

Oscar Zambrano · Augusto E. Rapalini · Federico M. Dávila · Ricardo A. Astini · Cecilia M. Spagnuolo

Received: 23 December 2009 / Accepted: 8 June 2010

Abstract Magnetostratigraphic and paleomagnetic studies on early Andean synorogenic strata (Del Crestón Fm.), in the Famatina Belt (28.7°S, 67.5°W) clarify details of chronology that permit calculation of sedimentation rates within the broken foreland of west Argentina. The Del Crestón Fm represents the first record of broken foreland sedimentation within the southern Central Andean belt and the earliest retroarc volcanic rocks exposed several hundred kilometers from the trench. Twenty-five out of 49 sites collected along the succession presented a primary remanence, as determined through positive fold and reversal tests. Correlation of the local magnetic polarity section with the global polarity time scale indicates that the sedimentation of Del Crestón Fm started at ~16.7 Ma and continued until ~14.5 Ma. The youngest strata are represented by conglomerates bearing abundant Lower Paleozoic granite boulders indicating unroofing of the crystalline basement within the NW Sierras Pampeanas. This result supports the hypothesis of an early broken foreland stage at these latitudes of the Andes, with involvement of the basement in deformation and coeval retroarc volcanism, common attributes of flat-subduction regimes. A mean site paleomagnetic direction of Dec: 6.3°, Inc: −43.6° (α95: 8.0°, $N = 24$) confirm our earlier intrepretation that the central part of the Famatina Belt within the Sierras Pampeanas did not undergo large vertical axes rotations since the Middle Miocene.

Keywords Magnetostratigraphy · Paleomagnetism · Central Andes · Cenozoic · Foreland basin

O. Zambrano · A. E. Rapalini (✉) · C. M. Spagnuolo
INGEODAV, Depto. Cs. Geológicas, F.C.E.yN., Universidad de Buenos Aires and CONICET, Pabellón 2, Ciudad Universitaria, C1428EHA Buenos Aires, Argentina
e-mail: rapalini@gl.fcen.uba.ar

F. M. Dávila · R. A. Astini
Laboratorio de Análisis de Cuencas-CICTERRA-CONICET, Cátedra de Estratigrafía y Geología Histórica, Facultad de Ciencias Exactas, Físicas y Naturales Universidad Nacional de Córdoba, Av. Velez Sarsfield 1611, 2° Piso, Of. 7, X5016GCA Córdoba, Argentina

Present Address:
O. Zambrano
Instituto Antártico Argentino, Buenos Aires, Argentina

Present Address:
C. M. Spagnuolo
IESGLO, Instituto de Sedimentología, Fundación Miguel Lillo, Miguel Lillo 251, T4000JFE San Miguel de Tucumán, Argentina

Introduction

Magnetostratigraphy is a technique widely used for stratigraphic correlation and relative geochronology (see Opdyke and Channell 1996). Its application to geological problems encompasses a varied field of investigations into basin analysis (e.g., Reynolds et al. 2001). In particular, it has been successfully applied in non-marine Cenozoic successions in foreland basin systems (e.g., Johnson et al. 1986; Reynolds et al. 1990; Homke et al. 2004; Sun et al. 2005; Fang et al. 2007). With the assistance of radiometric geochronologic techniques, magnetostratigraphy permits assignment of a "quasi-continuous" age to sedimentary strata based on the correlation of the local magnetostratigraphic column with the global polarity time scale (e.g., Gradstein et al. 2004). This aids in the calculation of accumulation rates that, in turn, may be interpreted in terms of the tectonic evolution of the basin. In particular, the high reversal rate of the Earth's magnetic field in the

Published online: 03 July 2010

Cenozoic (Gradstein et al. 2004) and the usually high sedimentation rates of many Cenozoic foreland basins (Jordan 1995) provide a strong potential for high-resolution magnetostratigraphic studies that have become routine in basin analysis.

The southern segment of the Central Andes is characterized by a complex volcanic and tecto-sedimentary evolution, both in time and space (e.g., Jordan et al. 1983, 1993, 2001; Marrett and Strecker 2000; Kay and Mpodozis 2002; Dávila and Astini 2007). This evolution has been recorded in numerous retroarc foreland basins and sub-basins, which contain thousands of meters of clastic continental deposits, frequently intercalated with pyroclastic products from the western volcanic arc (Ramos 1999). Detailed sedimentological and chronostratigraphic studies on these basins have permitted an understanding of the kinematics and timing of the Andes exhumation and uplift (e.g., Jordan et al. 1993). Andean magnetostratigraphy (e.g., McFadden et al. 1985; Johnson et al. 1986; Reynolds et al. 1990, 2001; Jordan et al. 1990; Malizia et al. 1995; Irigoyen et al. 2000; Re and Barredo 1993; Milana et al. 2003) in turn, has contributed greatly to unraveling the complex temporal and spatial evolution of the foreland during the Neogene.

Cratonward within the intermontane system of the Sierras Pampeanas of western Argentina, the magnetostratigraphic studies are scarce. In this region, within the Famatina belt, a thick Early Miocene synorogenic megasequence, known as the Del Crestón Formation (Dávila and Astini 2002, 2003a, b; Dávila et al. 2004), underlays the widespread Mio-Pliocene successions of the NW Sierras Pampeanas. This unit has been recently dated and interpreted to record the initiation of sedimentation within the Andean broken foreland (Dávila et al. 2004; Dávila and Astini 2007). This succession also records the magmatic broadening in the southern Central Andes, probably associated with the initiation of shallow subduction and changes in the convergence rates of the South American and Nazca plates (Dávila and Astini 2007; Dávila 2010).

In order to better constrain the age and accumulation rates of the Del Creston Formation and to compare its evolution with other foreland basin deposits of the southern Central Andes, a magnetostratigraphic study was carried out along a nearly complete exposure of this unit. The local magnetostratigraphic column allows bracketing the deposition age of this succession within the late Early to the early Middle Miocene. Paleomagnetic declinations suggest minor block rotation since the Miocene in this area of the westernmost broken foreland, which is in conflict with previous interpretations of paleomagnetic data from sites scattered across the region (de Urreiztieta et al. 1996; Aubry et al. 1996).

Geologic setting

In the flat-slab segment of the southern Central Andes (28°–33°S) (cf., Barazangi and Isacks 1976) and within the basement-involved Sierras Pampeanas province (broken foreland according to Jordan and Allmendinger 1986 and Jordan 1995), the Famatina belt extends for about 400 km between 27° and 31°S (Fig. 1). The structure of this region is characterized by doubly vergent, high-angle, basement thrusts (see Dávila and Astini 2002, 2003b; Ramos et al. 2002; Dávila 2003; Dávila et al. 2004). Two major basement uplifts bound the Angulos-Famatina valley (the Cordón de la Cumbre to the west and the Sierra de Paimán/Ramblones to the east), where several thousand meters of Cenozoic strata accumulated (Fig. 1b).

The Cenozoic stratigraphy of Famatina is composed of over 3,500-m-thick alluvial strata represented by the Del Crestón Formation, overlain by the Mio-Pliocene Angulos Group and the Pleistocene Santa Florentina Formation (Fig. 1b). The stratigraphy was separated into continental megasequences, represented from bottom to top by: (a) the lower section of the Lower Miocene Del Crestón Formation (ca. 17–16 Ma, MS1), (b) the upper section of the Del Crestón Formation (MS2), (c) the Middle Miocene Del Abra Formation and lower part of the Middle Miocene Del Buey Formation (MS3), (d) the upper part of the Middle Miocene Del Buey (MS4) and Santo Domingo formations (MS 4), (e) the Upper Miocene-Lower Pliocene El Durazno Formation (MS 5) and (f) the Plio-Pleistocene Santa Florentina Formation (for details on sedimentology and stratigraphy see Dávila and Astini 2007). In this work, we focus on the two megasequences recorded in the Del Crestón Formation, MS1 and MS2.

The lower megasequence MS1 (Fig. 1b, see also Fig. 6) is composed of a fine-grained tabular conglomerate overlain by saline playa-lake deposits (lower member of Dávila and Astini 2002) and by ~450 m of debris-flow-dominated alluvial-fan deposits (second member of andesite conglomerates of Dávila and Astini 2002), interpreted as lahar sequences (Dávila et al. 2004). The second upward thickening and coarsening megasequence MS2 begins with playa-lake fine-grained red beds overlain by sandy polymictic conglomerates (third member or sandy member of Dávila and Astini 2002), which are capped by 370 m of granite-rich, cobble to boulder conglomerate (fourth member) interpreted as prograding megafan deposits (Dávila and Astini 2002).

The overlying Angulos Group (Dávila 2005) is 1,942 m thick and represents three megasequences (MS3 to MS5) that record a complex Middle Miocene to Pliocene foreland evolution within the Famatina belt.

Jordan et al. (2001) and Ramos et al. (2002) constrained the "broken foreland stage", involving the study region, between 6.5 Ma and present. A similar model was recently

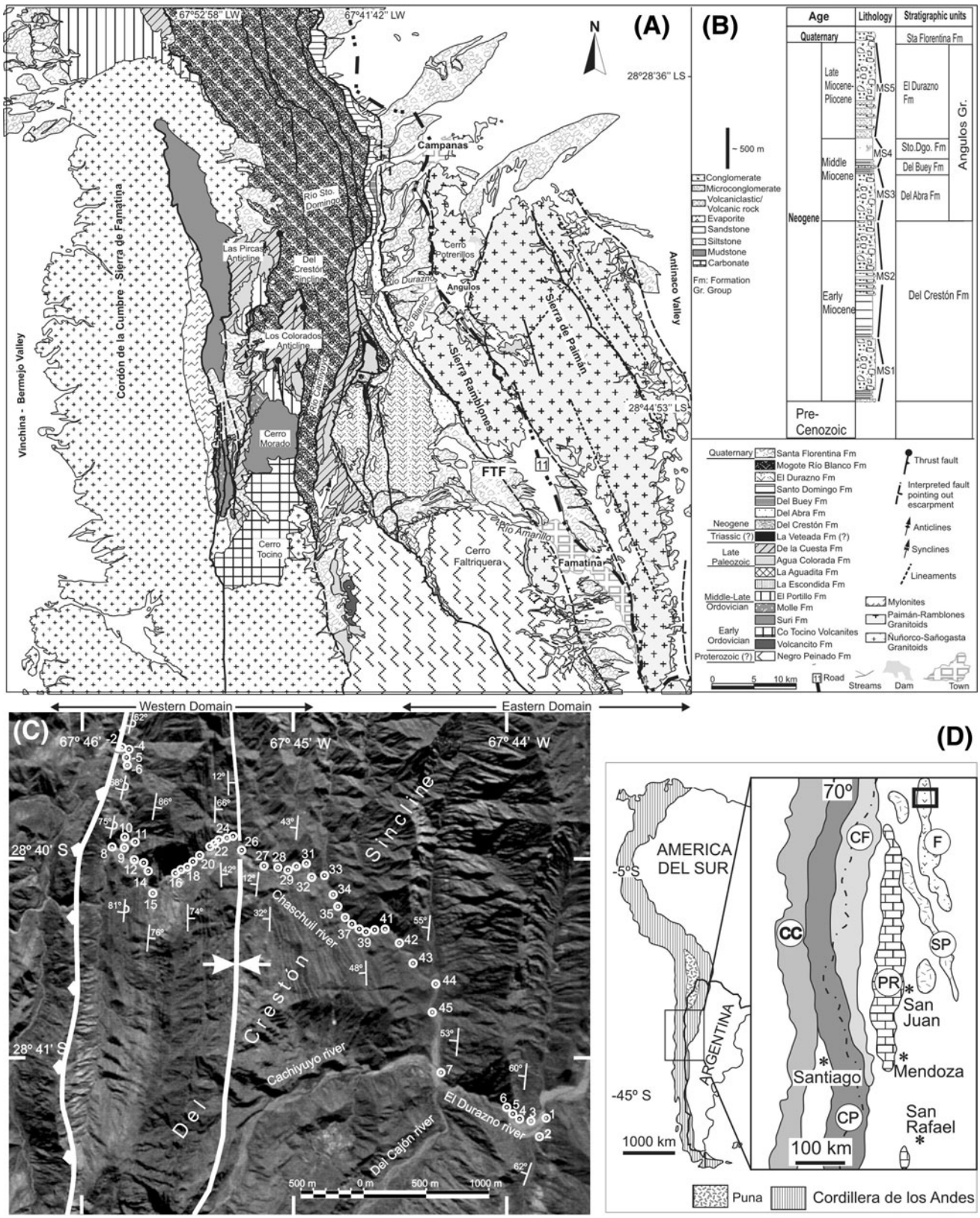

Fig. 1 **a** Geologic map of the central region of the Famatina belt and location of the study area. **b** General stratigraphic column for the Cenozoic of the Famatina Ranges including the five continental megasequences (MS1 to 5) defined by Davila and Astini (2007). **c** Satellite image of the Del Crestón syncline and distribution of paleomagnetic sampling sites. **d** Location of the study locality and main morphotectonic units of western Argentina and Chile (*CC* Cordillera de la Costa; *CF* Cordillera Frontal; *CP* Cordillera Principal; *F* Famatina; *P* Precordillera; *SP* Sierras Pampeanas Occidentales)

proposed by Carrapa et al. (2008), who suggested that the transition from thin-skinned to basement thrusting occurred contemporaneously along the Andean foreland (from the Eastern Cordillera in the north to the Bermejo Basin in the south) at ca. 6 Ma. Dávila and Astini (2007) and Dávila (2010), however, based on stratigraphically constrained compositional and paleocurrent analysis, interpreted that basement foreland partitioning would have begun much earlier in Famatina, likely as early as late Early Miocene (~17 Ma). Our magnetostratigraphic study permits a more precise dating of the Del Crestón succession supporting this notion of an early transition to the broken foreland stage in Famatina.

Paleomagnetic study and results

Forty-nine sites were located through the succession of the Del Crestón Formation across the Del Crestón syncline (Fig. 1). Sampling sites were located on both, east and west limbs. Twenty-seven were located along the eastern limb (over 1,600 m of stratigraphic thickness), whereas 22 along the western flank (over 1,000 m). The sampled interval encompasses the three lower members of the unit (the complete MS1 and the lower two-thirds of the MS2). Unfortunately, the upper coarse conglomerate member (fourth member) could not be sampled due to access problems to the outcrops and scarcity of suitable lithologies for paleomagnetic studies. Three 6–9-cm-long cores were collected at most sites with a portable gasoline-powered drill and oriented with both sun and magnetic compasses whenever possible. A few sites were sampled by means of two or three block samples. The bedding attitude was measured several times at each site (Table 1), and means were obtained for each. Bedding correction was performed by rotating the magnetic parameters an amount equal to the bedding dip along a horizontal axis coincident with the strike. No correction was taken for plunging of the syncline axis as this was computed to be less than 2° toward az. 184°.

Paleomagnetic processing was done at the INGEODAV paleomagnetic laboratory (Departamento de Ciencias

Table 1 Mean site paleomagnetic data for the Del Crestón Formation

Site	*n* (*N*)	Dec (°)	Inc (°)	*k* (α95)	Bedding correction	Dec* (°)	Inc* (°)
DC-5**	3	53.9	72.1		9°/112°	83.5	−34
DC-4	3	22.4	2.1		9°/112°	5.5	−13.5
DC-2	3	40.8	38.7		9°/118°	37.4	−41.0
DC1	3	178.9	35.9		181°/62°	212.8	17.2
DC2	3	317.3	−10.1		181°/62°	348.2	−43.0
DC3	2	355.2	−7.2		181°/62°	4.6	−8.3
DC4	3	160.2	13.8		181°/62°	184.1	24.4
DC5	2	338.0	−16.9		181°/62°	6.3	−27.6
DC6	3	318.7	−19.1		181°/62°	0.4	−45.5
DC7	1	310.0	−40.0		181°/53°	19.7	−59.9
DC8	3	235.8	−13.0		11°/105°	194.3	46.2
DC9	3	219.8	2.5		3°/98°	174.0	35.9
DC10	1	252.1	8.5		10°/91°	170.6	60.6
DC13	3	235.0	11.7		5°/86°	171.6	49.7
DC14	2	79.5	−17.7		11°/76°	358.7	−68.5
DC15	1	59.8	−32.4		11°/76°	338.3	−47.8
DC17	2	221.1	−1.5		0°/74°	195.6	38.4
DC19	2	59.7	−10.5		0°/74°	7.2	−59.8
DC20	2	227.0	−13.0		0°/74°	212.0	38.2
DC21	2	214.9	35.2		0°/66°	153.3	41.4
DC23	1	240.0	54.5		2°/42°	150.7	68.9
DC25	3	3.8	−61.4		350°/12°	341.3	−61.9
DC26	3	186.2	36.3		61°/5°	184.3	32.2
DC28	3	166.4	44.3		183°/32°	199.0	44.5
DC29	3	188.6	46.2		183°/32°	215.6	35.2
Mean in situ	(24)	22.4	−22.7	3.8 (17.5°)			
Mean after correction	(24)			14.8 (8.0°)		6.3	−43.6

n (*N*): number of samples (sites). *Dec**, *Inc**: declination and inclination after bedding correction. Bedding correction is expressed as strike azimuth and dip (in a direction 90° clockwise from strike). k and α95, Fisher's statistical parameters. ** Site not computed in the mean

Geológicas, Universidad de Buenos Aires, Argentina). Measurement of intensity and direction of the remanent magnetization was done with a 2G (DC-squids) cryogenic magnetometer. Measurement of bulk susceptibility was performed with a Bartington MS-2. AF demagnetization was done with a static 3-axis degausser attached to the magnetometer. Thermal demagnetization was performed with a dual-chamber furnace (ASC scientific) with an internal magnetic field under 10 nT.

One specimen per site was submitted to stepwise alternating field demagnetization in steps of 3, 6, 9, 12, 15, 20, 25, 30, 40, 50, 60, 80, 100 and 120 mT. Another specimen per site was submitted to stepwise thermal demagnetization in steps of 100, 150, 200, 250, 300, 350, 400, 450, 500, 550, 590, 620, 640, 660 and 680°C. Since thermal demagnetization proved to be more efficient than AF to discriminate different magnetic components, remaining specimens were submitted to thermal demagnetization in steps of 110, 200, 300, 350, 400, 450, 500, 550, 590, 620, 640, 660 and 680°C. Bulk susceptibility was measured after each demagnetization step in order to control possible chemical changes during experimental heating.

Paleomagnetic analyses were carried out by visual inspection of the demagnetization behavior through As-Zijderveld plots and demagnetization curves. Components were computed through principal component analysis (Kirschvink 1980) and accepted if defined by three or more consecutive steps and with maximum angular deviations under 15°. The basal member was sampled at sites DC1 to DC6 in the eastern limb (see Fig. 1) mostly formed by purple siltstones to fine-grained sandstones. Typical demagnetization behavior for most of these samples is provided by Fig. 2a. A single component with unblocking temperatures well over 600°C indicates that hematite is the magnetic carrier. However, few samples with a much lower unblocking temperature were also present (Fig. 2b). In some cases, both components with opposite polarities were isolated (Fig. 2c), suggesting a secondary, possibly viscous origin for the lower-temperature component.

With the exception of sites DC7, in the eastern limb, and DC-4 and DC-2 in the western limb, corresponding to thin red shale beds near the top of the second member, all the remaining sites were located within the third member. On the eastern limb, many sites of this member showed unstable magnetizations or presented an in situ low-temperature component, consistent with the present Earth Magnetic Field, suggesting a secondary (viscous?) magnetization. Therefore, along this flank, only sites DC26, 28 and 29 supplied remanence directions interpreted to be of primary origin based on a positive fold test. All remaining sites carriers of a primary remanence are located along the western limb of the Del Crestón syncline (Fig. 1). Typical remanence behaviors are illustrated in Fig. 2d–f. In most cases, remanence was isolated at temperatures under 500°C, suggesting titanomagnetites as the dominant mineralogy. However, a relatively minor contribution from hematite is inferred from persistent magnetizations over 600°C. In some cases, a secondary low-temperature component was isolated (Fig. 2d).

Mean site remanence directions were computed, both in situ and after correction for bedding attitude (Fig. 3, Table 1). In all sites, isolated components show consistent directions although due to the low number of samples per site ($n \leq 3$) no proper statistical evaluations of the within site consistency could be calculated. Comparison of Fig. 3a and b clearly show that the remanence is pre-folding. In Fig. 3c, all site directions have been plotted on the upper hemisphere, regardless of their polarity, after bedding correction to show the overall distribution. A positive result of the fold test is statistically confirmed by applying Enkin's test (Enkin 2003, Fig. 4). Stepwise unfolding (from −50 to 150%) produces maximum k at 94.6% unfolding ($k = 14.9$), which is statistically undistinguishable from 100% ($k = 14.8$). Application of a reversal test to the site remanence directions (McFadden and McElhinny 1988) gives a positive result of class "C" (angle between means of normal and reverse populations: 4.8°, critical angle: 17.5°). The positive fold and reversal tests suggest that the isolated remanence directions of Fig. 3 and Table 1 are likely primary.

Total angular dispersion of computed virtual geomagnetic poles from each site is 19.1°, which permits estimation of the between-site or field dispersion (McFadden et al. 1991) at 18°, slightly larger than predicted (around 16°) for the sampling latitude according to different models of paleosecular variation for the last 5 million years (McFadden et al. 1991; Johnson et al. 2008). However, the obtained value is consistent with the expected dispersion of VGPs for the interval 5–22.5 Ma (McFadden et al. 1991), suggesting that most or all directional dispersion can be attributed to the paleofield behavior.

In order to gain insight into the magnetic mineralogy, acquisition of isothermal remanent magnetization curves were obtained for representative samples of this formation. These experiments were carried out with an IH10-30 (ASC Scientific) impulse magnetizer, applying increasing fields along the z axis of 17, 29, 44, 61, 90, 150, 250, 350, 450, 600 and 1000 mT. The results are shown in Fig. 5. Most samples show the presence of two remanence-carrier minerals. The ferrimagnetic fraction (magnetite?) is present in most samples and tends to dominate the IRM acquisition curve. However, saturation is not obtained at fields under 1 T, indicating that an antiferromagnetic mineral, likely hematite, is also present. As pointed out above, the presence of both fractions also is evident in demagnetization diagrams. An exception to this pattern are

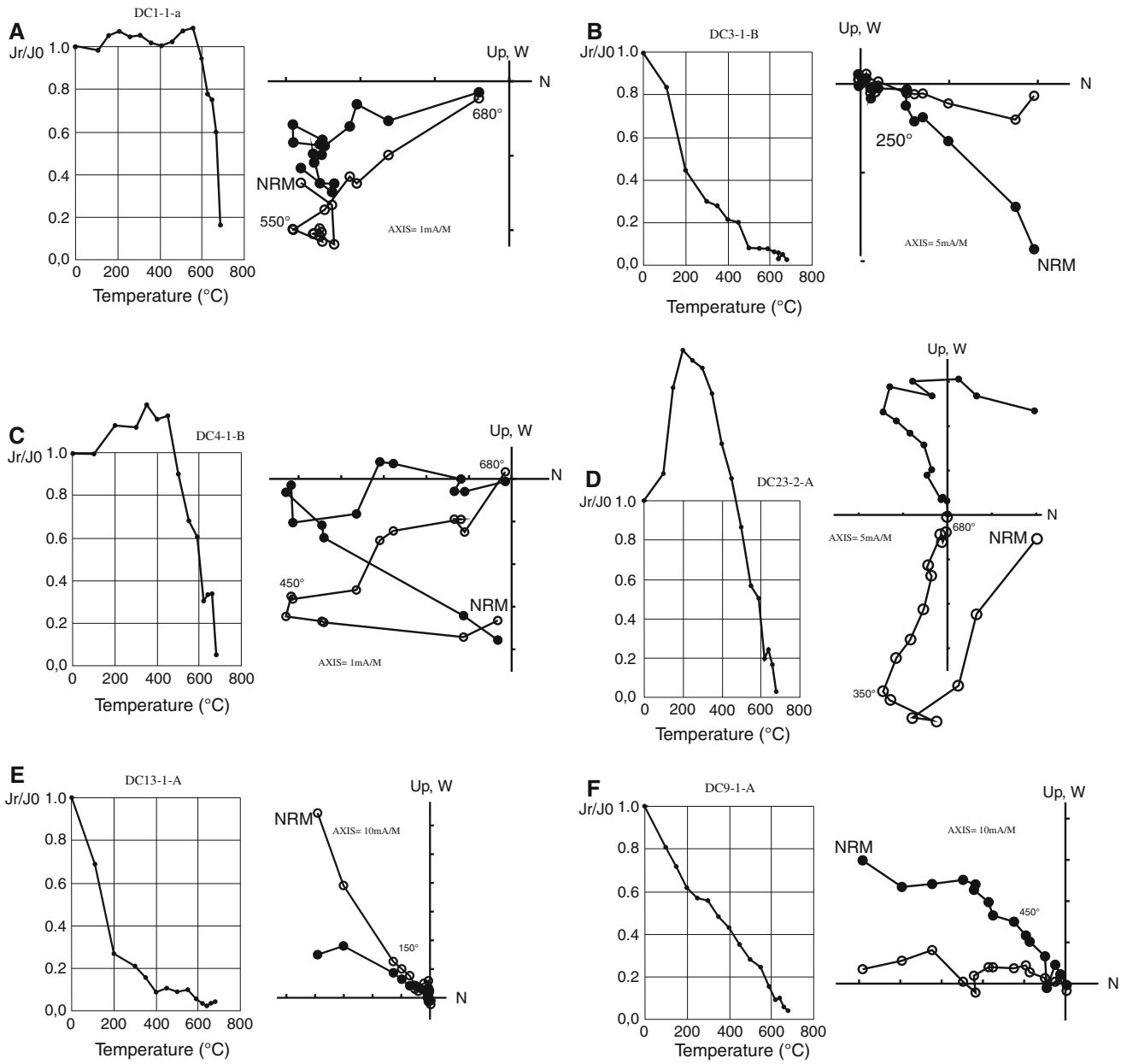

Fig. 2 Representative demagnetization plots for the Del Crestón Formation. Magnetic behavior during thermal cleaning is shown by intensity demagnetization curves and As-Zijderveld diagrams. Full (*open*) symbols indicate vectorial representations on the horizontal (*vertical*) plane. See descriptions in the text

samples DC1 and DC2 (lower member), which show a single antiferromagnetic phase with no evidence of magnetite. The fact that these sites recorded opposite polarities suggests a primary remanence. The IRM acquisition curves, from sites where a reliable remanence could not be obtained (DC32, DC40 and DC44), do not show a significantly different curve pattern, although they might carry a lesser amount of magnetite (see sample DC32)

Our results support a primary remanence in the Del Crestón Formation. The remanence polarity at each site can thus be used to construct a local magnetostratigraphic column. The mean remanence direction of all sites will assist us to analyze possible tectonic rotations around vertical axes that might have affected the studied succession.

Analysis and interpretation

The overall site mean direction, Dec: 6.3°, Inc: −43.6°, $\alpha 95$: 8.0° (see also Table 1), was compared with the expected direction for the sampling locality, according to

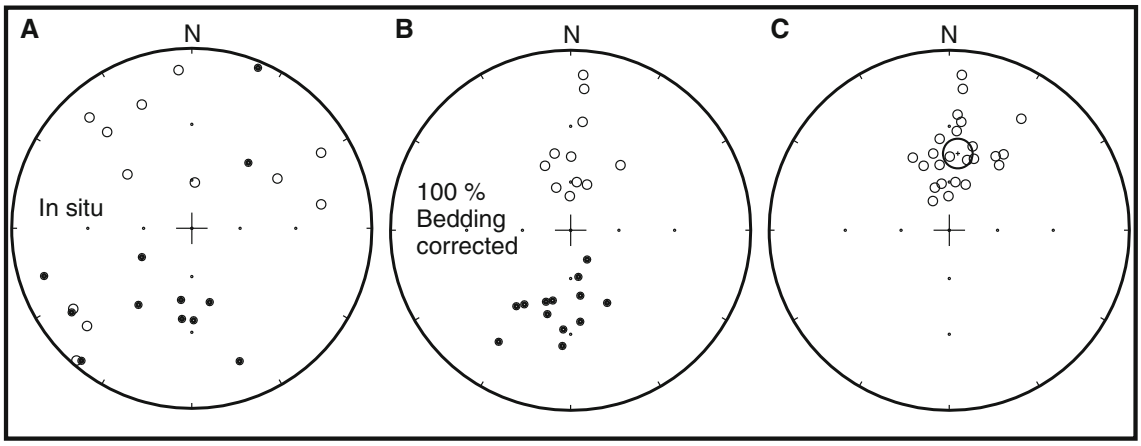

Fig. 3 **a** In situ mean site remanence directions for the Del Crestón Formation (Table 1), **b** idem after bedding correction, **c** idem B after inverting all positive directions to the upper hemisphere. Equal-area projection, open (*solid*) symbols mean negative (*positive*) inclinations

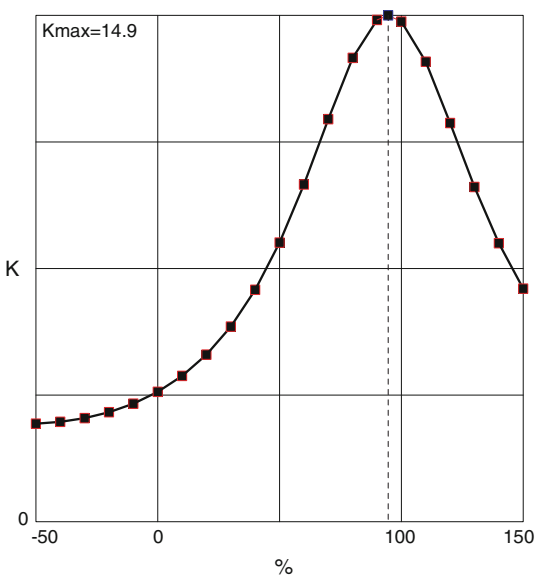

Fig. 4 Statistical parameter *k* versus % of unfolding for the Del Crestón site remanence directions. Percentage of unfolding for maximum *k* is shown as a *dashed line*. Note that this is attained at virtually 100% unfolding, implying a positive tilt test

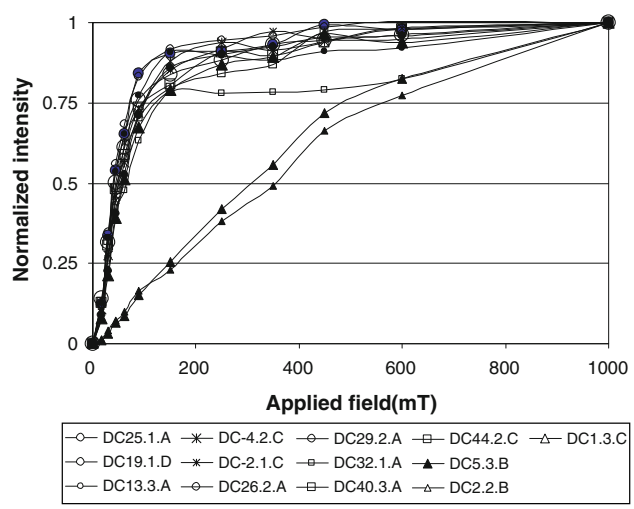

Fig. 5 Normalized isothermal remanent magnetization acquisition curves for representative samples of the Del Crestón Formation. Note the dominance of a ferrimagnetic phase (magnetite?) in most samples, as well as lack of saturation under 1 tesla. *Different symbols* correspond to samples from different limbs and members. More references and discussion in the text

the 15 Ma reference paleomagnetic pole for South America as computed by Besse and Courtillot (2002). Applying the algorithm of Beck (1989), a statistically insignificant value of 8.9° ± 9.4° clockwise rotation and a small inclination anomaly of 9.2° ± 6.9° were obtained. This confirms lack of significant Andean tectonic rotations in the area, as already indicated by Spagnuolo et al. (2008) based on Late Paleozoic paleomagnetic data from the same locality. This is also consistent with kinematic analyses on minor faults along the major thrusts of the region (Dávila 2003). However, de Urreiztieta et al. (1996) and Aubry et al. (1996) suggested widespread clockwise rotations involving most of the south Central Andean foreland since the Neogene. Our results, together with the spatial distribution of paleomagnetic data published by Aubry et al. (1996), indicate that there would have been several large areas that did not undergo such tectonic rotations. Therefore, the rotations associated with the formation of the Bolivian orocline would have not involved regions further south or, eventually, deformation might have been transferred along strike-slip zones within the northern Sierras Pampeanas region. However, we notice that our results are incapable of detecting tectonic rotations <10°.

The small, but statistically significant, inclination anomaly is likely due to the inferred detrital character of the remanent magnetization (e.g., Butler 1992; Tauxe 2000) carried by the ferrimagnetic fraction (magnetite)

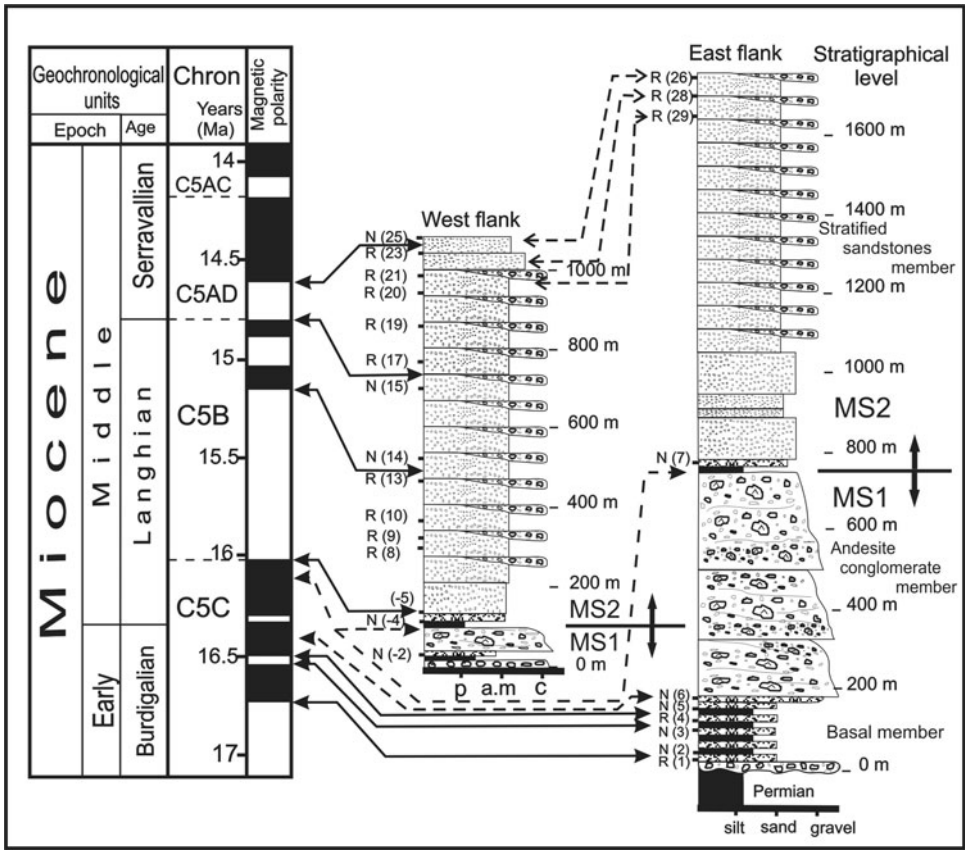

Fig. 6 Stratigraphic distribution of sites and magnetic polarities on the Del Crestón Formation along both flanks of the Del Crestón syncline. Correlation of magnetic polarities with the global polarity time scale (Gradstein et al. 2004). Note lack of polarity definition along most of the upper section of the eastern flank. More discussion in the text

or to sediment compaction (e.g., Deamer and Kodama 1990).

Figure 6 shows the distribution of magnetic polarity of the Del Crestón Formation on both flanks of the syncline. The sites where no remanence directions were isolated are not shown. Moreover, most sites along the sandy member of the eastern flank failed to provide reliable polarity information. However, the polarity succession along this unit could be determined by combining the data from the lower member, along the eastern flank, with the sampled section along the western limb. Despite significant westward thining of the lower conglomerate deposits (MS1, Fig. 6), correlation of different stratigraphic levels exposed along both limbs of the Del Crestón syncline can be unambiguously obtained in the field (Dávila and Astini 2003a), from the top sampled levels (DC-25 and 26, DC-28 and 29), close to the syncline hinge, downwards. The paleomagnetic results allow determining unambiguously the polarity for 24 of 25 sites. Site DC-5 shows an intermediate polarity that we interpret as a likely record of an Earth magnetic field reversal. Figure 6 also shows the proposed correlation between the magnetic polarity recorded in the Del Creston Fm, in the Sierra de Famatina, with the global polarity time scale (GPTS, Gradstein et al. 2004). Dávila et al. (2004) provided an important maximum depositional age for the lower conglomeratic member (MS1) of the Del Crestón Fm of ca. 17 Ma, based on Ar–Ar dating (on amphibole) of two andesitic clasts collected near the base of such deposits along the same section sampled in our study. At that stratigraphic level, the conglomerate is texturally an oligomictic, unsorted breccia, basically composed of andesitic clasts and boulders. Dávila et al. (2004) have found that the structures, textures and fabric indicate that these conglomerates are sedimentary gravity-flow deposits of local derivation whose transport was facilitated by relatively high gradient slopes. Genetically, they have been classified as lahar deposits. A proximal volcanic source is evident for the volcanogenic breccias of the Del Crestón Formation, which are typical of those developed adjacent to volcanic edifices. Although no primary andesite lava flows have been documented in the study area, Sosic (1972) described andesite flows along strike to the north that interfinger with similar conglomeratic facies. These considerations indicate that the age of the andesitic boulders must closely correspond to deposition of the conglomerate. These ages are essential for our magneto correlation. Supplementary minimum ages come from the overlying Angulos Group, recently constrained between the Middle to Late Miocene to Pliocene (Tabbutt 1990; Dávila 2005; Barreda et al. 2006; Martina et al. 2006). In particular, the palinologic study of Barreda et al. (2006) indicates a Middle Miocene age for the base of the

El Buey Fm., close to the top of MS3 (Fig. 1), more than 500 m up from the top of the Del Crestón Fm. and over 1,000 m up from the stratigraphically highest levels sampled in our study. Fossil fauna found in calcareous levels at the middle section of the El Buey Fm. (Dávila 2005) also are indicative of a Middle Miocene age. Considering this, it is highly unlikely that the top levels of the Del Crestón Fm be younger than 14 Ma. These age constraints permitted a successful magnetostratigraphic correlation that was achieved following the standard methodology for these studies (Opdyke and Channell 1996).

Considering the age constraints, the local magnetostratigraphic column obtained from the Del Crestón Formation must be fitted within the polarity intervals of the global polarity time scale (Gradstein et al. 2004) between ca. 17 and 14 Ma. (Fig. 6). A single correlation scheme was selected as it provided a reasonable adjustment, while alternative correlations yielded unrealistic or unlikely solutions. The correlation selected is described below.

The lower member is represented by four polarity intervals (R-N-R-N) that suggest relatively frequent reversals. Therefore, we correlate this member with the first four polarity intervals within subchron C5C (between 16.7 and 16.4 Ma), whereas the overlying andesite conglomerate member correlates with the long normal interval of this subchron (between 16.4 and 16.0 Ma). Despite the scarce number of sampling sites located in this member, this interpretation is based on a composite interval formed by the normal polarities recorded at the base and top of this member on the eastern flank (DC6, DC7) and the same polarity found in the main body and at the top of this member on the western limb (Fig. 6).

The remaining polarity succession is based mainly on sites from the western limb. The transitional polarity recorded at site DC-5 (third member) is interpreted as the normal to reverse transition, from subchron C5C to C5B. The following four sites, distributed over ~350 m of stratigraphic succession, show a reverse polarity consistent with the long (0.8 Myr) interval of reverse polarity recorded by subchron C5Br. A transition to a normal polarity interval is interpreted to occur between sites DC13 and DC14. The latter and DC15, located ~200 m upward, show normal polarity. This large stratigraphic gap, with no data, let us to interpret that the two normal polarity and one reverse polarity interval that correspond to C5B.2n, C5B.1r and C5B.1n occur within this interval. (i.e., the short reverse interval is missing from our records, Fig. 6). Otherwise, to attribute both DC14 and DC15 to correspond to the short normal interval slightly older than 15 Ma, and the following section to the short reverse interval immediately on top, would lead to unrealistically high accumulation rates. The polarity change from C5B to C5AD subchrons (at ~14.9 Ma) is interpreted to occur between sites DC15 and DC17. This is followed by ~300 m of reverse polarity (sites DC17, DC19, DC20, DC21 and DC23), which correlates with chron C5ADr (between ~14.8 and 14.6 Ma). This reverse polarity is also observed in the three sites exposed close to the top of Del Creston Fm along the eastern flank (sites DC26, DC28 and DC29). Transition to interval C5ADn is interpreted to occur between sites DC23 and DC25. This is the uppermost sampled site.

Based on this analysis, we suggest that the three lower members of the Del Creston Fm accumulated between ~16.7 and 14.5 Ma. Since the upper conglomerate member was not sampled, the time span for deposition of the whole formation can be constrained to no less than 2.2 Myr.

Considering this new constraint for the uppermost section of the Del Creston Fm at around 14.5 Ma, the major unroofing of the Paleozoic basement of the Famatina belt might have occurred slightly after the date previously proposed (Dávila et al. 2004). This also suggests that the main deposition along the deep Andean foredeep (Vinchina Fm and correlatives, Jordan et al. 2001), exposed to the west of the study region, occurred contemporaneously with the uplifting of the basement-involved thrust belt of Famatina expressed in mega-sequence 2 and its capping granite boulder conglomerate.(Dávila and Astini 2003c). This new constraint allows confirmation that an early shallow-subduction regime developed along the southern Central Andes (Dávila et al. 2004; Dávila and Astini 2007), contributing to the discussion on the timing of the foreland partitioning and arrival of flat slabs in Argentina [Early-Middle Miocene (Dávila 2010) versus latest Miocene to Pliocene (Carrapa et al. 2010)].

Unpublished magnetostratigraphic studies on the Vinchina Fm (Re 2008) indicate a sudden increase in the sedimentation rates at ~14 Ma, coincidently with our deductions of major uplift in Famatina. Our new chronology also supports previous interpretations (Dávila and Astini 2007) on the preservation of the >10 km Vinchina foredeep. The uplifting of the Famatina basement range (>400 km along strike) would have created a structural damming effect to eastward sediment dispersal, favouring along-strike flow and aggradation within an intermontane foreland basin developed between the Cordillera and exhumed highs of the broken foreland.

Since several reversals of the Earth Magnetic Field were recorded within the Del Creston Fm, sedimentary accumulation rates were calculated from the lower sequence (MS1) to the lower part of the upper sequence (MS2). Results are plotted in Fig. 7. While an average accumulation rate of 0.5 mm/year was calculated for the basal section of the lower member, a 2.0 mm/year is suggested for the upper section (volcanogenic lower conglomerate

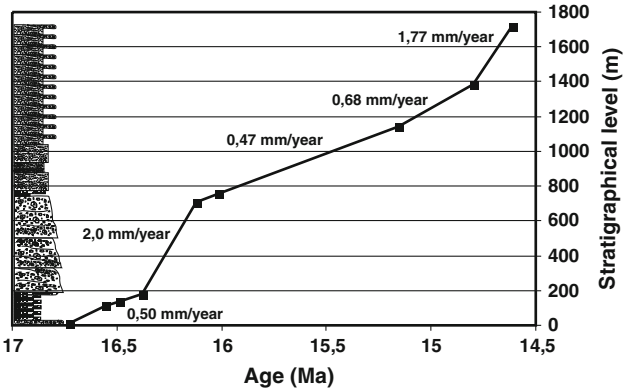

Fig. 7 Sedimentary accumulation rates for the Del Crestón Formation obtained from the magnetostratigraphic correlation

member). They correspond to the first upward coarsening megacycle defined by Dávila and Astini (2002, 2003a, b). The second megacycle (MS2) starts ca. 16.1 Ma with a depositional rate of 0.47 mm/year that increases up section to 1.77 mm/year near the top. It is noteworthy that sedimentation rates increase with coarser accumulation and or volcanogenic input as suggested also for the younger and overlying Angulos Group (Martina et al. 2006).

Conclusions

Magnetostratigraphy from 25 sites, collected along the three lower members in the Del Crestón Formation (western Sierras Pampeanas), allowed us to bracket between the late Early to early Middle Miocene the sedimentation ages for this unit. A correlation of the local magnetic polarity column to the global polarity time scale indicates that sedimentation of the two coarsening-upward megacycles occurred between 16.7 and 14.5 Ma. Although the uppermost granite-rich coarse conglomerate was not sampled, age constraints on the overlying Del Abra and Del Buey Formations (Barreda et al. 2006) suggest that deposition of the whole the Del Crestón sediments was completed by ca. 14 Ma. Inferred sedimentary rates are consistent with grain-size trends, indicating that higher rates are associated with coarser more proximal sources. Moreover, predominance of granite composition within the upper member is a strong evidence for coeval exhumation of local basement.

The mean remanence direction shows that large areas of Famatina did not undergo significant crustal block rotations (<10°) since the Miocene, as supported by other studies (Dávila 2003; Spagnuolo et al. 2008). This suggests that rotations associated with the Bolivian orocline might have not involved the western Sierras Pampeanas region.

The major participation of basement in thrusting would have been likely around 14.5 Ma, slightly more recently than proposed by Dávila and Astini (2007), but significantly earlier than Carrapa et al. (2010) hypothesis. This result is consistent with earlier development of shallow subduction and basement partitioning at these latitudes. The early broken foreland stage, recorded in the Famatina ranges (Dávila and Astini 2007), would have been contemporaneous with thick sedimentation recorded in the Vinchina foredeep, exposed further west, at the foothill of the Cordilleran belts. This would agree with a previous suggestion, based on clast composition and provenance studies, that the preservation of the tens of kilometers of alluvial successions was driven by the creation of basement topographic barriers.

Acknowledgments This study was financed through grants UBA-CyT X183 and PIP-CONICET 5783 from the Universidad de Buenos Aires and CONICET (Argentina). Further funding by FONCyT, CONICET and SECyT-UNCor to FMD and RAA is gratefully acknowledged. Mabel Mena helped us with some statistical analyses, and Rubén Somoza critically reviewed an earlier version of the manuscript. Thorough and constructive comments by T. Jordan and W. MacDonald significantly improved the original manuscript.

References

Aubry L, Roperch P, Urreiztieta M, Rossello E, Chauvin A (1996) Paleomagnetic study along the southeastern edge of the Altiplano-Puna Plateau: neogene tectonic rotations. J Geophys Res 101(B8):17883–17900

Barazangi M, Isacks BL (1976) Spatial distribution of earthquakes and subduction of the Nazca Plate beneath South America. Geology 4:686–692

Barreda VD, Ottone EG, Dávila FM, Astini RA (2006) Edad y paleoambiente de la Formación del Buey (Mioceno), Sierra de Famatina, La Rioja, Argentina: evidencias sedimentológicas y palinológicas. Ameghiniana 43:215–226

Beck ME Jr (1989) Block rotations in continental crust: examples from western North America. In: Kissel C, Laj C (eds) Paleomagnetic rotations and continental deformation. Kluwer Academic Publishers, Dordrecht

Besse J, Courtillot V (2002) Apparent and true polar wander and the geometry of the geomagnetic field over the last 200 Myr. J Geophys Res 107(11):2300. doi:10.1029/2000JB000050

Butler RF (1992) Magnetic domains to geologic terranes. Blackwell Scientific Publications, Cambridge 319 pp

Carrapa B, Hauer J, Schoenbohm L, Strecker MR, Schmitt AK, Villanueva A, Sosa Gómez J (2008) Dynamics of deformation and sedimentation in the northern Sierras Pampeanas: an integrated study of the Neogene Fiambalá basin, NW Argentina. Geol Soc Am Bull 120:1518–1543

Carrapa B, Hauer J, Schoenbohm L, Strecker MR, Schmitt AK, Villanueva A, Sosa Gómez J (2010) Dynamics of deformation and sedimentation in the northern Sierras Pampeanas: an integrated study of the Neogene Fiambalá basin, NW Argentina: reply. Geol Soc Am Bull 122:950–953

Dávila FM (2003) Transecta estratigráfica-estructural a los 28°30′–28°54′ de latitud Sur, Sierra de Famatina, provincia de La Rioja, República Argentina. Tesis Doctoral Inédita, Facultad de

Ciencias Exactas, Físicas y Naturales, Universidad Nacional de Córdoba, 516 pp

Dávila FM (2005) Revisión estratigráfica y paleoambientes del Grupo Angulos (Neógeno), Sierra de Famatina, La Rioja, Argentina: su significado en el relleno del antepaís fragmentado. Revista de la Asociación Geológica Argentina 60:32–48

Dávila FM (2010) Dynamics of deformation and sedimentation in the northern Sierras Pampeanas: an integrated study of the Neogene Fiambalá basin, NW Argentina: discussion. Geol Soc Am Bull 122:946–949

Dávila FM, Astini RA (2002) Estratigrafía de la Formacón Del Crestón, Sierra de Famatina, Argentina: Sedimentación paleógena en el antepaís andino. Revista de la Asociación Geológica Argentina 57:463–483

Dávila FM, Astini RA (2003a) Discordancias progresivas en los depósitos pre-neógenos del Famatina (Formacón Del Crestón), La Rioja, Argentina y su implicancia en la cronología evolutiva del antepaís andino. Revista de la Asociación Geológica Argentina 58:109–116

Dávila FM, Astini RA (2003b) Early Middle Miocene broken foreland development in the southern Central Andes: evidence for extension prior to regional shortening. Basin Res 15:379–396

Dávila FM, Astini RA (2003c) Las eolianitas de la sierra de Famatina (Argentina): interacción paleoclima-tectónica en el antepaís fragmentado andino central durante el Mioceno Medio? Revista Geológica de Chile 30:187–204

Dávila FM, Astini RA (2007) Cenozoic provenance history of synorogenic conglomerates in western Argentina (Famatina belt): implications for Central Andean foreland development. Geol Soc Am Bull 119:609–622

Dávila FM, Astini RA, Jordan TE, Kay SM (2004) Early Miocene andesite conglomerates in the Sierra de Famatina, broken foreland region of western Argentina, and documentation of magmatic broadening in the south-central Andes. J South Am Earth Sci 17:89–101

de Urreiztieta M, Gapais D, Le Corre C, Cobbold PR, Rosello E (1996) Cenozoic dextral transpression and basin development at the southern edge of the Puna Plateau, northwestern Argentina. Tectonophisics 254:17–39

Deamer GA, Kodama KP (1990) Compaction-induced inclination shallowing in synthetic and natural clay-rich sediments. J Geophys Res 95(B4):4511–4529

Enkin RJ (2003) The direction-correction tilt test: an all-purpose tilt/fold test for palaeomagnetic studies. Earth Planet Sci Lett 212:151–166

Fang X, Zhang W, Meng Q, Gao J, Wang X, King J, Song C, Dai S, Miao Y (2007) High-resolution magnetostratigraphy of the Neogene Huaitoutala section in the eastern Qaidam Basin on the NE Tibetan Plateau, Qinghai Province, China and its implication on tectonic uplift of the NE Tibetan Plateau. Earth Planet Sci Lett 258:293–306

Gradstein FM, Ogg JG, Smith AG (2004) A geologic time scale 2004. In: FM Gradstein, JG Ogg, AG Smith (eds) pp. 610. Cambridge University Press, Cambridge, UK, April 2005. ISBN 0521781426

Homke S, Vergés J, Garcés M, Emami H, Karpuz R (2004) Magnetostratigraphy of Miocene–Pliocene Zagros foreland deposits in the front of the Push-e Kush Arc (Lurestan Province, Iran). Earth Planet Sci Lett 225:397–410

Irigoyen MV, Buchan KL, Brown RL (2000) Magnetostratigraphy of neogene Andean foreland-basin strata, lat 33° S, Mendoza Province, Argentina. Geol Soc Am Bull 112:803–816

Johnson PA, Jordan TE, Johnson NM, Naeser CW (1986) Magnetic polarity stratigraphy, age and tectonic setting of foreland basin, San Juan province, Argentina. Int Assoc Sedimentol Special Publ 8:63–75

Johnson CL, Constable CG, Tauxe L, Barendregt R, Brown LL, Coe RS, Layer P, Mejia V, Opdyke ND, Singer BS, Staudigel H, Stone DB (2008) Recent investigations of the 0–5 Ma geomagnetic field recorded by lava flows. Geochem Geophys Geosyst 9(4):Q04032. doi:10.1029/2007GC001696

Jordan TE (1995) Retroarc foreland basins. In: Burby CJ, Ingersoll RV (eds) Tectonics of sedimentary basins. Blackwell Scientific Publications, Cambridge, pp 331–362

Jordan TE, Allmendinger RW (1986) The Sierras Pampeanas of Argentina: a modern analog of Rocky Mountain foreland deformation. Am J Sci 286:737–764

Jordan TE, Isacks BL, Allmendinger RW, Brewer JA, Ramos VA, Ando CJ (1983) Andean tectonics related to the geometry of the subducted Nazca Plate. Geol Soc Am Bull 94:341–361

Jordan TE, Rutty PM, McRae LE, Beer JA, Tabbutt KD (1990) Magnetic polarity chronostratigraphy of the Miocene Rio Azul section, Precordillera thrust belt, San Juan Province. Argent J Geol 98:519–539

Jordan TE, Allmendinger RW, Damanti JF, Drake RE (1993) Chronology of motion in a complete thrust belt: the Precordillera, 30°–31° S, Andes Mountains. J Geol 101:137–158

Jordan TE, Schlunegger F, Cardozo N (2001) Unsteady and spatially variable evolution of the Andean Neogene Bermejo Foreland Basin, Argentina. J South Am Earth Sci 14:775–798

Kay SM, Mpodozis C (2002) Magmatism as a probe to the Neogene shallowing of the Nazca plate beneath the modern Chilean flat-slab. J South Am Earth Sci 15:39–57

Kirschvink JL (1980) The least squares line and plane and the analysis of paleomagnetic data. Geophys J Roy Astron Soc 62:699–718

Malizia DC, Reynolds JH, Tabutt KD (1995) Chronology of Neogene sedimentation, stratigraphy, and tectonism in the Campo de Talampaya region, La Rioja province, Argentina. Sediment Geol 96:231–255

Marrett R, Strecker M (2000) Response of intracontinental deformation in the central Andes to late Cenozoic reorganization of South American Plate motions. Tectonics 19:452–467

Martina F, Dávila FM, Astini RA (2006) Mio-Pliocene volcaniclastic deposits in the Famatina ranges, southern Central Andes: a case of volcanic controls on sedimentation in broken foreland basins. Sediment Geol 186:51–65

McFadden PL, McElhinny MW (1988) The combined analysis of remagnetization circles and direct observations in paleomagnetism. Earth Planet Sci Lett 87:161–172

McFadden PL, McElhinny MW, Merrill RT (1985) Non-linear processes in the geodynamo—palaeomagnetic evidence. Geophys J 83:111–126

McFadden PL, Merrill RT, McElhinny MW, Lee S (1991) Reversals of the earth's magnetic field and temporal variations of the dynamo families. J Geophys Res 96(B3):3923–3933

Milana JP, Bercowski F, Jordan T (2003) Paleoambientes y magnetoestratigrafía del Neógeno de la Sierra de Mogna, y su relación con la Cuenca de Antepaís Andina. Revista de la Asociación Geológica Argentina 58:447–473

Opdyke ND, Channell JET (1996) Magnetic stratigraphy. Academic press, San Diego, CA 346 pp

Ramos VA (1999) Rasgos estructurales del territorio argentino. 1. Evolución tectónica de la Argentina. In: Caminos R (ed) Geología Argentina. Instituto de Geología y Recursos Minerales, Anales 29 (24):715–784, Buenos Aires

Ramos VA, Cristallini EO, Pérez DJ (2002) The pampean flat-slab of the Central Andes. J South Am Earth Sci 15:59–78

Re G (2008) Magnetoestratigrafías del NO argentino (entre 27° y 31° S) aplicadas al análisis de la deformación andina, y su relación con la subducción de la placa de Nazca durante el Cenozoico tardío. Universidad de Buenos Aires, PhD Thesis, 283 pp (unpublished)

Re H, Barredo SP (1993) Esquema de correlación magnetoestratigráfica de formaciones terciarias aflorantes en las provincias de San Juan, La Rioja y Catamarca. Revista de la Asociación Geológica Argentina 48(3–4):241–246

Reynolds JH, Jordan TE, Johnson NM, Damainti JF, Tabbutt KD (1990) Neogene deformation of the flat-slabduction segment of the Argentine-Chilean Andes: magnetostratigraphic constraints from Las Juntas, La Rioja province, Argentina. Geol Soc Am Bull 102:1607–1622

Reynolds JH, Hernández R, Galli C, Idelman B (2001) Magnetostratigraphy of the Quebrada La Porcelana section, Sierra de Ramos, Salta province, Argentina. Initial age limits on the regional Neogene lithostratigraphy and uplift of the southern Sierras Subandinas. J South Am Earth Sci 14:681–692

Sosic MVJ (1972) Descripción geológica de la Hoja 14d, Tinogasta (provincias de Catamarca y La Rioja). Dirección Nacional de Geología y Minería, Boletín 129, 60 p. Buenos Aires

Spagnuolo CM, Rapalini AE, Astini RA (2008) Palaeomagnetic confirmation of Palaeozoic clockwise rotation of the Famatina Ranges (NW Argentina): implications for the evolution of the SW margin of Gondwana. Geophys J Int 173(2):63–78

Sun Z, Yang Z, Pei J, Ge X, Wang X, Yang T, Li W, Yuan S (2005) Magnetostratigraphy of Paleogene sediments from northern Qaidam Basin, China: implications for tectonic uplift and block rotation in northern Tibetan plateau. Earth Planet Sci Lett 237:635–646

Tabbutt KD (1990) Temporal constraints on the tectonic evolution of Sierra de Famatina, Argentina using the fission track method to date synorogenic clastic sequences. J Geol 98:557–566

Tauxe L (2000) Paleomagnetic principles and practice. Springer, NewYork 312 pp